International Journal of Education and Science Research Review
E-ISSN 2348-6457
Volume-10, Issue-5 Sep - Oct – 2023
P-ISSN 2349-1817
www.ijesrr.org
Email- editor@ijesrr.org

CORROSION PREVENTION: ELECTROCHEMICAL METHODS FOR METAL PROTECTION IN VARIOUS ENVIRONMENTS.

Dr. Munesh Meena

Assistant Professor

SCRS Govt P G College Sawai Madhopur

ABSTRACT

Metals are susceptible to a wide variety of methods and circumstances, which is highlighted by the phenomena of corrosion, which is a worldwide phenomenon that causes irreparable damage to metals through chemical and electrochemical interactions. As a result, producers are required to find a compromise between creating products at a low cost and ensuring that they have optimal corrosion resistance, taking into account the specific locations in which they will be used, and doing so without sacrificing industry standards. Within the scope of this review, a variety of variables and kinds of metallic corrosion are briefly examined. In addition to this, it explores a variety of approaches that are implemented with the intention of preventing and minimizing the occurrence of the phenomenon.

Keywords:- *Corrosion prevention, metal protection.*

INTRODUCTION

An irreversible damage to the surface of a metal that results in the transformation of a pure metal into more chemically stable forms such as sulfides, oxides, hydroxides, and other similar compounds is what we mean when we talk about corrosion. Over the course of this process, chemical and electrochemical processes take place on the surface of the metal in an environment that is corrosive. This environment can be solid, liquid, or gas. The corrosive media in question is the one that allows for the classification of corrosion as either dry or wet.

The reversal of the process of extracting metals from their ores, which occur naturally in the form of ore, is the process of metallic corrosion. Therefore, energy is required in order to extract metals from ores. When metals travel through their life cycle, however, they have a tendency to get oxidized, which means they return to their initial states. Corrosion tendencies of metals are proportional to the amount of energy required to extricate them from their respective environments.

In most cases, the corrosion of metallic materials is caused by an electrochemical process. It is common practice for the process to involve the utilization of an electrolyte, which facilitates the movement of ions (both cations and anions) within the system and gives rise to anodic and cathodic processes. When two distinct metals are present in an electrolyte, the metal with a lower level of nobleness becomes the anode and corrodes, while the metal with a higher level of nobleness becomes the cathode and is protected. As electrons move from the anodic metal to the cathodic metal, the flow of electrons occurs. Both of the metals are susceptible

to corrosion, but the one that has a higher reduction potential, or a higher position in the electrochemical series, is the more likely to be affected by corrosion.

Furthermore, regardless of the morphology of the metal damage, metallic corrosion can manifest itself in a variety of different ways. It has been suggested by Singh that corrosion can manifest itself as a widespread surface attack, which gradually reduces the thickness of the metal. It is also possible for it to manifest itself as isolated corrosion in particular regions or along weak lines, such as grain boundaries, which is influenced by changes in resistance to an environment that is corrosive against corrosion.

Metallic corrosion is characterized by its multifaceted aspect, which highlights the fact that metals are susceptible to a wide range of mechanisms and variables that might cause corrosion. As a result, this paper provides an in-depth discussion of the various types of corrosion that can occur in metallic materials. Furthermore, it delves into the topic of a variety of tactics that are made with the intention of preventing and minimizing corrosion.

OBJECTIVES

1. To study corrosion prevention.
2. To study Pre-treatment of Metals

Factors of corrosion

This section provides an emphasis on the many different elements that contribute to the corrosion of metallic materials. The elements that are investigated include the purity of the metal, the characteristics of the surface film, the properties of corrosive materials, the temperature, the humidity of the air, and the pH levels among others. In order to conduct a thorough investigation into the corrosion process in metals, it is essential to have a solid understanding of these factors.

- **Purity of the Metal**

  According to Harsimran et al., the rate of corrosion normally increases with the increased accumulation of impurities. This is because the impurities produce miniature electrochemical cells in which the anodic component suffers corrosion. For example, zinc that contains impurities like iron (Fe) or lead (Pb) is subject to a more rapid rate of corrosion.

- **Nature of Surface Film**

  In an atmosphere that contains oxygen, every metal will eventually form a thin layer of metal oxide on its surface. The "specific volume ratio," which is the ratio of volumes between the metal oxide and the metal, influences the impact of this surface coating. This ratio is the ratio of volumes between the metal and the metal oxide. A decrease in the rate of oxidation is associated with a specific volume ratio that is higher. One example is that nickel, cobalt, and tungsten each have specific volume ratios of 1.6, 2.0, and 3.6, respectively. Consequently, even when subjected to higher temperatures, tungsten demonstrates the lowest rate of oxidation.

- **Nature of Corrosive Product**

  If the product that is formed is soluble in the medium that is corrosive, then the rate of corrosion will occur more quickly. Furthermore, if the corrosive product is volatile, it will evaporate upon production, leaving the surface of the metal vulnerable to additional attack and making the corrosion process even more severe.

- **Temperature**

  It is anticipated that the rate of corrosion will approximately double for every 100-degree increase in temperature. Corrosion is accelerated with higher temperatures. Muslim et al. conducted studies on aluminum and copper at temperatures of 25 degrees Celsius and 50 degrees Celsius, with pH values of 4.8, 7, and 8.2 correspondingly. They discovered that the corrosion rates of aluminum and copper decreased with increasing pH and rose with higher temperatures. In most cases, an exponential curve is used to illustrate the relationship between temperature and the growth in corrosion; however, there are a number of instances that demonstrate a more complicated relationship, as changes in temperature can also modify the impact of other elements.

- **Humidity of the Air**

  The rate of corrosion is substantially impacted by relative humidity, which exhibits a dramatic increase after it beyond a particular threshold that is referred to as the critical humidity. When this threshold is exceeded, there is a discernible increase in the damage caused by corrosion. An enhanced susceptibility of the oxide film to absorb moisture, which in turn leads to further electrochemical corrosion, is responsible for the increased corrosion that occurs when the humidity level is raised. In addition, the water that is required for the electrolyte, which is necessary for the construction of an electrochemical cell, is provided by the moisture that is present in the atmosphere.

- **pH**

  One of the most important factors that determines the rate of corrosion is the pH level, with increased corrosion rates being associated with lower pH levels. For example, when compared to alkaline or neutral media, acidic environments, which are characterized by a pH that is lower than 7, exhibit more corrosiveness. When it comes to noble metals like gold and platinum, the rate of corrosion is remarkably low and shows only a small effect on the pH of the solution. Despite the fact that noble metals are generally resistant to corrosion, they are not typically utilized for common uses due to the high cost of these metals. When compared to neutral solutions, the rate of corrosion for other metals, such as aluminum, zinc, and lead, is significantly higher in acidic and alkaline mediums. This is the case regardless of whether the medium is neutral or acidic. The fact that the oxides of these metals are soluble in both acidic and alkaline conditions provides an explanation for this phenomenon.

Pre-treatment of Metals

Performing a comprehensive cleaning of the metal surface is a crucial step that must be taken before any protective measures are used. Oily and greasy surface layers can be successfully dissolved through the process of degreasing, which is often carried out with the help of a volatile organic solvent such as trichloroethylene.

In addition, acid pickling is an additional approach that can be used to remove scale, which is a complementary method to mechanical cleaning. An adequate preparation of the metal surface, which includes the removal of oils and grease, is required prior to the application of any coating. This can be accomplished by washing the surface with an alkaline solution.

Research methodology

MS Sample and Test Electrolyte

MS, which is also known as ordinary steel and low carbon steel, was subjected to both electrochemical and non-electrochemical processes. MS is considered to be one of the most desired materials in the industry due to its availability, physical qualities, and affordability. For the purpose of this inquiry, mechanical spectroscopy was utilized in accordance with the following percentage composition: (C = 0.22, Mn = 0.05, Si = 0.38, S = 0.05, P = 0.09, Al = 0.01, and the remaining iron). The surface area of the samples that were exposed was one centimeter squared, and prior to testing, they were mechanically abraded using emery papers of several grades (120, 220, 400, 600, 800, 1500, and 2000 grade). After being washed with distilled water, having acetone used to remove oil, being dried, and being stored in vacuum desiccators, the coupons were taken. By diluting Analar grade hydrochloric acid at a concentration of 37% with ultra-pure water, the test electrolyte with a concentration of 1 M HCl was created. Each and every measurement was carried out a minimum of three times in order to achieve a suitable level of repeatability.

Inhibitor elaboration

Three different substances were added to a medium that included 1H-pyrazolo [3,4-d]pyrimidin-4(5H)-one (0.5 g, 3.67 mmol) dissolved in DMF (30 mL). These substances were 3-bromoprop-1-ene (1.4 mL, 7.4 mmol), potassium carbonate (1.02 g, 7.4 mmol), and a catalytic amount of tetra-nbutylammonium bromide (0.1 g, 0.4 mmol). For a period of forty-eight hours, the complete contents of the preparation were subjected to agitation, and the reaction was investigated using thin layer chromatography. Following the filtration of the mixture, the solvent was separated using a vacuum cleaner. After the solvent was vaporized under low pressure, the residue that was recovered was chromatographed on a silica column using a mixture of hexane and ethyl acetate with a volume-to-volume ratio of 4:6. The same eluent is responsible for the recrystallization process. Using 1H NMR, 13C, IR, and mass, the product that was produced was analyzed and described.

The identification of the light yellow solid compound was carried out (56 % yield), 1H NMR (DMSOd6):δ4.59 (dd, 2H, N5CH2, 3 J = 4.59, 4 J = 4.57 Hz), 4.89 (dd, 2H, N1CH2, 3 J = 4.9, 4 J = 4.68 Hz), 4.94 (m, 2H, =CH2, 3 J = 4.9, 4 J = 4.6), 5.1 (m, 2H, =CH2, 3 J = 5.1, 4 J = 4.8), 5.95 (m, 1H, =CH, 3 J = 5.93, 4 J =5.63), 6.02 (m, 1H, =CH, 3 J = 5.91, 4 J = 5.71 Hz), 8.10 (s, 1H, H-3), 8.34 (s, 1H, H-6). By using 13C nuclear magnetic resonance (DMSO-d6), the following chemical shifts were observed: δ 47.46 (N5-CH2), 49.56 (N1-CH2), 105.46 (C, C-3a), 117.79 (=CH2), 118.02 (=CH2), 133.88 (=CH2), 135.08 (CH, C-3), 151.06 (CH, C-6), 151.62 (C, C-7a), and 156.60 (CO, C-4). C11H12N4O (M + H) + m/z: 217.11 according to the HRMS (APPI) calculation.

Weight loss (wl)

The gravimetric tests were carried out in a double glass cell that was fitted with a cooling condenser that was regulated by a thermostat. 50 milliliters was the total volume of the solution. All of the specimens were in the

shape of rectangles. After the trials were over, they were rinsed thoroughly with ethanol while being subjected to ultrasonography, and then they were weighed. The experiments were carried out three times, and the average value of the weight loss (WL) was recorded after each repeated experiment. For the purpose of calculating the average corrosion rate (CR) expressed in mg cm−2 h, we were able to utilize the WL. The following equation was utilized in order to estimate the values of the corrosion rate:

$$CR = \frac{Weight\ loss\ (\mathrm{mg})}{\text{area}\ (\mathrm{cm^2}) \times time\ (\mathrm{h})} \quad \textbf{(1)}$$

Applying the following equation, we were able to determine the proportion of protective efficiency of WL tests based on the corrosion rate:

$$E_{\mathrm{WL}} = \frac{CR_{\mathrm{uninhibt}} - CR_{\mathrm{inhibt}}}{CR_{\mathrm{uninhibt}}} \times 100 \quad \textbf{(2)}$$

The corrosion rates in the absence of an inhibitor (anti-corrosion agent) and the corrosion rates in the presence of an inhibitor are denoted by the symbols CRuninhibit and CRinhibit, respectively.

To determine the surface coverage (θ) values, the equation that was used to calculate them is as follows:

$$\theta = \frac{E_{\mathrm{WL}}}{100} \quad \textbf{(3)}$$

Electrochemical measurements

With a water bath that was thermostated, all of the electrochemical tests were carried out at 303 degrees Kelvin. There were three electrodes installed in the electrochemical cell. A saturated calomel electrode (SCE) served as the reference electrode in this experiment. Both the platinum electrode and the MS electrode had a surface area of one square centimeter, and the platinum electrode was utilized as an auxiliary electrode. The MS electrode was used as the working electrode. The open circuit potential (OCP), potentiodynamic polarization curves (PDP), and electrochemical impedance spectroscopy (EIS) analysis were all included in the electrochemical tests that were carried out. For the purpose of carrying out these studies, a Volta lab potentiostat was utilized. Using the selected circumstances indicated above, the Tafel lines were measured. The electrode potential was applied at a slew rate of 0.5 mV/s, and the electrode potential ranged from -800 mV to -200 mV with regard to the corrosion potential. The measurements were carried out under the parameters mentioned above. In contrast, EIS testing were carried out at OCP with ten points per decade, using an AC voltage of ten millivolts peak to peak. The frequency range that was used for these tests was from one hundred kilohertz to ten millihertz. Plots of impedance are presented using the Nyquist and Bode representations here.

Computational theoretical studies

- **Computational method (dft techniques)**

All of the chemical computations of PPD were carried out by utilizing the natural bond orbital (NBO) analysis, which was carried out by use of the DFT electronic structure program Gaussian 16 Rev C.01. On the basis of B3LYP/6-31G(d,p) set in corrosive acid medium, the PPD in the isolated and neutral form as well as the complete complexes were minimized. This was accomplished through sophisticated calculation. We were able to discover the elements of quantum chemistry, such as EHOMO and ELUMO, which are helpful in elucidating the chemical characteristics of the Fe-(PPD) complex. In addition, the energy gap, denoted as ΔEg, was determined using the equation ΔEg = EHOMO − ELUMO. This energy gap ultimately defines the reactivity of the entire complex that was produced. The purpose of this work is to explain the relationship that exists between the findings of the experiments and the quantum chemical descriptors for the neutral form and the complexes that are found in various active centers.

- **Monte carlo/saa simulation**

The Monte Carlo simulation, which was paired with the simulated annealing algorithm (SAA), was executed by employing three sequential heating ramps, each of which consisted of 15 × 10−3 steps. In order to achieve findings of exceptional quality, the convergence threshold was established at 0.015 Å, 0.5 kcal/mol.Å, and 10−3 kcal/mol, respectively, for displacement, force, and energy. In order to determine the configuration with the lowest energy, the adsorption energy with the lowest energy, and any other essential information regarding the energy of the system, the adsorption location software makes use of the Metropolis sampling Monte Carlo approach.
The adsorption energy Eads is calculated by adding the deformation energy Denergy, which is the energy of the system as long as the optimization of the geometry is finished, to the rigid adsorption energy RAE, which is the energy of the system before the optimization of the geometry. There is a second set of geometry optimization that takes place when the PPD in hydrochloric acid medium is introduced to the surfaces of the Fe (100), Fe (110) and Fe (111) that are being investigated.
In order to provide a broad surface area for the interaction with a single inhibitor, the crystallographic planes of pure iron (100), pure iron (110) and pure iron (111) were extended to a super-cell size of 6 × 6 × 6. The calculation of the adsorption (interaction) energies for {PPD / Fe (110), Fe (110) and Fe (110)} complexes was realized through the utilization of the pure iron surface docking technique. The Ewald summation method and the atom-based summing approach were the two methods that were preferred for analyzing electrostatic and Van der Waals interactions, respectively. The COMPASS force field was utilized, and the calculations for this component were carried out with the assistance of the Adsorption Locator tools that are included in the Dassault systems program known as Biovia Material Studio 2020. An implementation of the COMPASS FF was carried out in order to compute the intermolecular interaction energies for the PPD that was docked on the surface of the pure Fe in a three-dimensional simulated crystal structure consisting of Fe (100), Fe (110), and Fe (111) − (Lx = Ly = 35/Lz = 40) having periodic boundary conditions. Following that, a vacuum slab with a thickness of 10 Å was constructed on top of the iron (100), iron (110) and iron (111) surfaces. It is possible to locate the simulation specifics on the technique of Monte Carlo/SAA in the publications that were published in the past.

- **SEM inspection**

Scanning electron microscopy (SEM) pictures were captured using the equipment provided by FEI (model: FEI-Quanta 650) with an acceleration energy of 20 kV for the purpose of conducting surface morphological examinations of both unfettered and inhibited MS samples subjected to 10−3 M PPD

inhibitor in 1 M HCl. Before moving on to the characterisation phase, the tests were carried out using an immersion that lasted for twenty-four hours.

Results and Discussion

Weight Loss Measurements (WL)

When it comes to determining the rate of corrosion, the weight loss strategy is another typical method. According to a number of research investigations, it is a potent instrument that can be used to estimate the amount of metal that has been lost. In Table 1, the WL data of specimens that were placed in a solution of 1 M HCl at 303 K are presented, both without and with varying quantities of the organic component that was introduced.

Table 1. Corrosion ratio and the % of protective effect on specimens following 6 h of exposure with and without PPD.

C (M)	CR (mg cm^{-2} h^{-1})	E_{WL} (%)	θ
Blank	0.600	– –	– –
10^{-3}	0.037	94	0.94
10^{-4}	0.062	90	0.90
10^{-5}	0.142	76	0.76
10^{-6}	0.252	58	0.58

In Table 1, it is evident that the rate of the corrosion process decreased, and the efficiency of the PPD protector improved as the concentrations of the compound under study increased (EWL = 94% at 10−3 M). It is because of the increased surface coverage that occurs with increasing concentrations of the molecule that is being tested that pyrazolo pyrimidine behaves in this manner in 1 M HCl. Adsorption onto the metal surface is one possible explanation for this phenomenon. Adsorption means that the test compound can be adsorbed onto the metal surface as a result of the interaction between the electron pairs of the nitrogen and oxygen atoms that are present in the protective agent and the metal surface. The presence of unoccupied low-energy orbitals in the MS atoms, as can be seen in the transition group metals, makes this process easier to carry out.

OCP Measurements

When there is no net current flowing through the cell, the opportunity current potential (OCP) is the potential of the working electrode in relation to the reference electrode. It is essential to ensure that the OCP remains stable before proceeding with the potentiodynamic polarization and EIS procedures.

The stability of the open circuit potential is shown in Figure 1 for all curves that are about 800 seconds. This indicates that 900 seconds is more than sufficient for the system to obtain a stable open circuit potential than 800 seconds. There was not much of a difference in the personality of OCP when PPD was present compared to when it was not present. The reason for this is that the surface metal activities of the inhibited and non-inhibited examples are slightly different from one another. A drop in OCP at the beginning of the experiment shows that the oxide layer that was generated by the air on the electrode dissolves in the acidic liquid over time. It is possible that the production of insoluble Fe (III) oxide, which ultimately results in a passive state on MS, is responsible for a later modest increase in potential of the material. The creation of a protective layer

of inhibitor on the metal surface can be explained by the fact that the OCP shifts to a more positive value when the observed concentrations of PPD are added to a solution of 1 M HCl. This displacement can be explained by the study. In addition, it is worth noting that when the concentration is 10−4 M, the OCP decreases rapidly towards cathodic values over time. This may be attributed to the dissolution of corrosion products, and it is also likely due to the fact that the PPD adsorption process on the electrode surface follows slow kinetics, which is similar to the weak PPD adsorption. In the case of 10−3 M, the OCP undergoes a change to a more positive value after a duration of 200 seconds, and it typically becomes stable after 380 seconds. It is possible that this indicates the rapid creation of a protective layer that has adsorbed on the surface of the sample. This layer will protect the sample from attacks by the aggressive medium and will eventually improve its resistance to corrosion in an HCl solution. As a result, it is possible to assert that PPD is able to slow down the processes that take place on the surface of the MS, specifically the oxidation of iron and the reduction of hydrogen ions in 1 M hydrochloric acid.

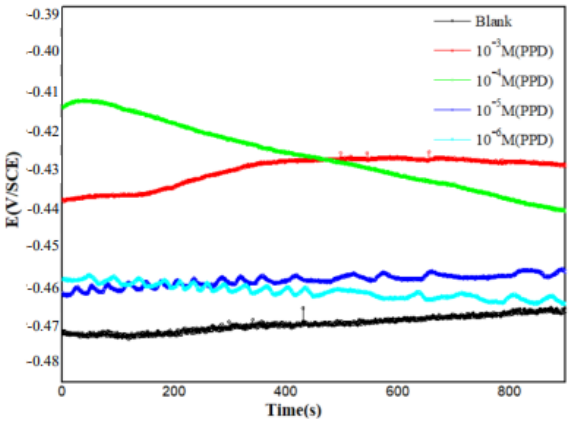

Figure 1. Chrono-potentiometric (zero current) curves for steel in 1 M HCl without and with different concentrations of PPD at 303 K.

CONCLUSION

In order to prevent the negative consequences of corrosion, which is a global phenomenon that affects materials, particularly metals and alloys, it is necessary to implement efficient mitigation measures. There are many different types of corrosion that occur as a consequence of the inherent characteristics of the metal and the corrosive environment. These types of corrosion include regionalized corrosion, stress corrosion, intergranular corrosion, galvanic corrosion, erosion, waterline corrosion, and biological corrosion. General or uniform corrosion is also included in this category. There are a variety of strategies that have been put into practice and documented in order to combat or resist corrosion in metals. As a result of taking into consideration the particular settings in which the materials will be used, manufacturers are required to strike a compromise between the development of materials that are both cost-effective and ensure that they have optimal corrosion resistance. At the same time, it is still a struggle to meet the norms and rules of the industry while simultaneously optimizing the performance of the material against corrosion.

REFERENCES

1. Redkina, G. V., Sergienko, A. S., & Kuznetsov, Y. I. (2020). Hydrophobic and anticorrosion properties of thin phosphonate-siloxane films formed on a laser textured zinc surface. International Journal of Corrosion and Scale Inhibition, 9(4), 1550-1563.

2. Biryukov, A. I., Kozaderov, O. A., Galin, R. G., Zakharyevich, D. A., &Zhivulin, V. E. (2020). Details of the mechanism of dissolution of iron-zinc coatings based on the δ-phase in acidic media. International Journal of Corrosion and Scale Inhibition, 9(4), 1477-1489.

3. Harsimran, S., Santosh, K., & Rakesh, K. (2021). Overview of corrosion and its control: A critical review. Proc. Eng. Sci, 3(1), 13-24.

4. Kuznetsov, Y. I. (2020). Triazoles as a class of multifunctional corrosion inhibitors. Review. Part II. 1, 2, 3-Benzotriazole and its derivatives. Iron and steels. International Journal of Corrosion and Scale Inhibition, 9(3), 780-811.

5. Balangao, J. K. B., Podiotan, F. J. C., Ambolode, A. E. C., & Anacleto, N. M. (2022). Isothermal reduction smelting of mixed chromite-laterite samples with coconut charcoal as reductant under argon atmosphere in a vertical electric arc furnace. International journal of mechanical engineering and technology, 13(5), 46-53.

6. Pal, M. K., & Lavanya, M. (2022). Microbial influenced corrosion: understanding bioadhesion and biofilm formation. Journal of Bio-and TriboCorrosion, 8(3), 76.

7. Hanoon, M., Zinad, D. S., Resen, A. M., &AlAmiery, A. A. (2020). Gravimetrical and surface morphology studies of corrosion inhibition effects of a 4-aminoantipyrine derivative on mild steel in a corrosive solution. International Journal of Corrosion and Scale Inhibition, 9(3), 953-966.

8. Kharanzhevsky, E. V., Reshetnikov, S. M., Efimov, A. V., Gil'mutdinov, F. Z., &Krivilev, M. D. (2020). Application of some inhibitors for improving the corrosion resistance of ceramic coatings deposited on non-alloy steel by short-pulse laser treatment. International Journal of Corrosion and Scale Inhibition, 9(1), 44-55.

9. Yimyai, T.; Thiramanas, R.; Phakkeeree, T.; Iamsaard, S.; Crespy, D. Adaptive Coatings with Anticorrosion and Antibiofouling Properties. Adv. Funct. Mater. 2021, 31, 2102568. [CrossRef]

10. Zhang, Q.H.; Hou, B.S.; Li, Y.Y.; Zhu, G.Y.; Lei, Y.; Wang, X.; Liu, H.F.; Zhang, G.A. Dextran 665 derivatives as highly efficient green corrosion inhibitors for carbon steel in CO2-saturated 666 oilfield produced water: Experimental and theoretical ap-proaches. Chem. Eng. J. 2021, 424, 130519. [CrossRef]

11. Ma, I.A.W.; Ammar, S.; Kumar, S.S.A.; Ramesh, K.; Ramesh, S. A concise review on 695 corrosion inhibitors: Types, mechanisms and electrochemical evaluation studies. J. Coat. Technol. Res. 2022, 19, 241–268. [CrossRef]

12. Huang, H.; Fu, Y.; Li, F.; Wang, Z.; Zhang, S.; Wang, X.; Wang, Z.; Li, H.; Gao, F. Orderly 702 self-assembly of new ionic copolymers for efficiently protecting copper in aggressive sulfuric acid solution. Chem. Eng. J. 2020, 384, 123293.

13. Jeyaram, R.; Elango, A.; Siva, T.; Ayeshamariam, A.; Kaviyarasu, K. Corrosion protection of silane based coatings on mild steel in an aggressive chloride ion environment. Surf. Interfaces 2020, 18, 100423.

14. Li, W.; Tan, B.; Zhang, S.; Guo, L.; Ji, J.; Yan, M.; Wang, R. Insights into triazole derivatives as potential corrosion inhibitors in CMP process: Experimental evaluation and theoretical analysis. Appl. Surf. Sci. 2022, 602, 154165.

15. El Ouasif, L.; Laourayed, M.; Benhiba, F.; Boudalia, M.; El Ghoul, M.; Achour, R.; Bellaouchou, A.; Guenbour, A.; Warad, I. Experimental and Theoretical Approaches for Interfacial Adsorption of Novel Long Chain Benzimidazolium Derivatives for Mild Steel Protection in 1 M HCl Medium. Anal. Bioanal. Electrochem. 2021, 13, 12–32. Available online: www.researchgate.net/publication/354582558 (accessed on 30 December 2022).

16. Echihi, S.; Benzbiria, N.; Belghiti, M.E.; El Fal, M.; Boudalia, M.; Essassi, E.M.; Guenbour, A.; Bellaouchou, A.; Tabyaoui, M.; Azzi, M. Corrosion inhibition of copper by pyrazole pyrimidine derivative in synthetic seawater: Experimental and theoretical studies. Mater. Today Proc. 2020, 37, 3958–3966.

17. El-Katori, E.E.; El-Saeed, R.A.; Abdou, M.M. Anti-corrosion and anti-microbial evaluation of novel water-soluble bis azo pyrazole derivative for carbon steel pipelines in petroleum industries by experimental and theoretical studies. Arab. J. Chem. 2022, 15, 104373.

18. Verma, C.; Saji, V.S.; Quraishi, M.A.; Ebenso, E.E. Pyrazole derivatives as environmental benign acid corrosion inhibitors for mild steel: Experimental and computational studies. J. Mol. Liq. 2020, 298, 111943.

19. Jasmin, A.S.; Rashid, K.H.; AL-Azawi, K.F.; Khadom, A.A. Synthesis of a novel pyrazole heterocyclic derivative as corrosion inhibitor for low-carbon steel in 1M HCl: Characterization, gravimetrical, electrochemical, mathematical, and quantum chemical investigations. Res. Eng. 2022, 15, 100573.

20. Sehmi, A.; Ouici, H.B.; Guendouzi, A.; Ferhat, M.; Benali, O.; Boudjellal, F. Corrosion inhibition of mild steel by newly synthesized pyrazole carboxamide derivatives in HCl acid medium: Experimental and theoretical studies. J. Electrochem. Soc. 2020, 167, 155508.